Journal of Sound and Vibration (2000) **238**(3), 459–480
doi:10.1006/jsvi.2000.3154, available online at http://www.idealibrary.com on IDEAL®

CORIOLIS COUPLING EFFECTS ON THE VIBRATION OF ROTATING RINGS

R. Eley, C. H. J. Fox and S. McWilliam

School of Mechanical, Materials, Manufacturing Engineering and Management, University of Nottingham, University Park, Nottingham NG7 2RD, England

(*Received* 7 *December* 1999, *and in final form* 22 *May* 2000)

The vibration properties of a ring subjected to angular velocity components applied simultaneously about three mutually perpendicular axes are investigated. Ring structures have potential applications as multi-axis rate sensors and hence the effects of angular velocity on the vibration properties are practically important. Coriolis coupling between in-plane and out-of-plane displacements of a ring due to angular velocity applied about axes in the plane of the ring, and about the polar axis of the ring, allow it to be used as a multi-axis rate sensor. Equations of motion are derived for the rotating ring. The combinations of in-plane and out-of-plane displacement patterns for which Coriolis coupling is present are investigated and the corresponding natural frequencies and mode shapes of the rotating ring are derived. Simple analytical expressions are developed for a number of special cases and some numerical examples are presented. The effect of small imperfection on the natural frequencies of the rotating ring is also considered.

1. INTRODUCTION

The range of applications for low-cost rate-sensors (rate-gyroscopes) is large and rapidly expanding in fields as diverse as automotive safety and navigation, defence and bio-mechanics. A single-axis vibrating-structure rate sensor is already commercially available that utilizes the in-plane vibration modes of a small silicon ring [1], which is readily manufactured in large quantities using micro-machining techniques [2].

Rate sensors are often used in applications in which there is a need to measure angular velocity about two or three axes simultaneously (e.g., roll, pitch and yaw). A novel multi-axis sensor based on a vibrating ring structure is potentially capable of sensing angular velocity components applied simultaneously about three mutually perpendicular axes [3]. This is achieved by using Coriolis coupling between in-plane and out-of-plane displacements of a ring in which a forced vibration is maintained. The principles of operation of such a sensor are described in reference [4].

The aim of this paper is to present an analysis of the effects of Coriolis coupling on the free vibration of a ring which is rotating about axes in the plane of the ring, as well as the polar axis. This analysis may be regarded as a pre-requisite for the forced vibration case, which is important for rate-sensor design. In rate-sensor applications, the applied rates of turn are always three or four orders of magnitude smaller than the relevant structural natural frequencies. In these circumstances, the effect of centrifugal loading is negligible and the Coriolis coupling is the dominant effect which modifies the vibration behaviour.

0022-460X/00/480459 + 22 $35.00/0

Many other workers have considered the dynamics of rings that are spinning about the polar axis, see, for example, references [5–8], often placing emphasis on the effects of centrifugal loading in rapidly rotating rings. The authors of the present paper are unaware of any other published analysis dealing with the effects on vibration of rotation applied about axes in the plane of the ring, as well as the polar axis.

2. ANALYSIS

It is useful to begin by noting that the modes of flexural vibration of non-rotating rings of uniform rectangular cross-section may be classified as either in-plane or out-of-plane modes. They occur in degenerate pairs, with equal natural frequencies, at a mutual angle of $\pi/2p$ where p is the number of nodal diameters; see Figures 1 and 2 (a list of notation is given in Appendix B). If the ring has dimensional imperfection [9, 10], or is manufactured from an anisotropic material [11] there may be splits in the frequency pairs. For operation as a rate gyro, these splits must ideally be reduced to a minimum, often using some form of frequency trimming [12] involving the addition or removal of material. In the present paper, the equations of motion will initially be derived by assuming the ring to be perfectly symmetrical, but the effects of imperfection will be represented in the final equations of motion.

Consider now the case of a flexible ring, as shown in Figure 3. The ring is uniform and isotropic and is subjected to applied angular velocity components, Ω_X, Ω_Y and Ω_Z acting axes Ox, Oy and Oz respectively, which are fixed in the undeformed ring. For the ring to be used as a practical rate sensor, it must be supported in some way. This can be achieved by using a number of support legs in the plane of the ring [1]. The supports are designed to have effective stiffness and mass values that are small compared to those of the ring so that, in the relevant flexural modes, the elastic deformation of the assembly is dominated by the ring. For simplicity of presentation, the supports are neglected in the following analysis.

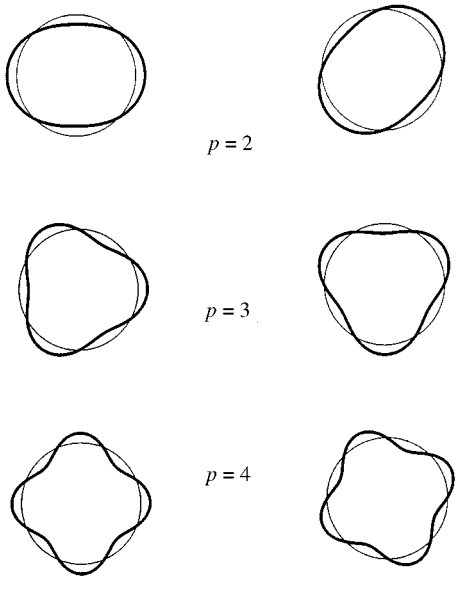

Figure 1. In-plane modes of non-rotating ring with $p = 2$, 3, 4 nodal diameters.

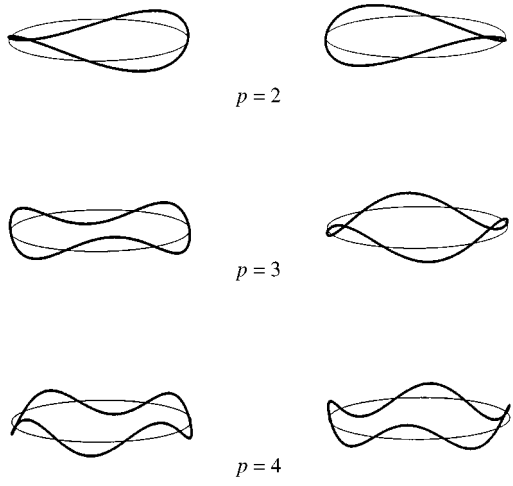

Figure 2. Out-of-plane modes of non-rotating ring with $p = 2, 3, 4$ nodal diameters.

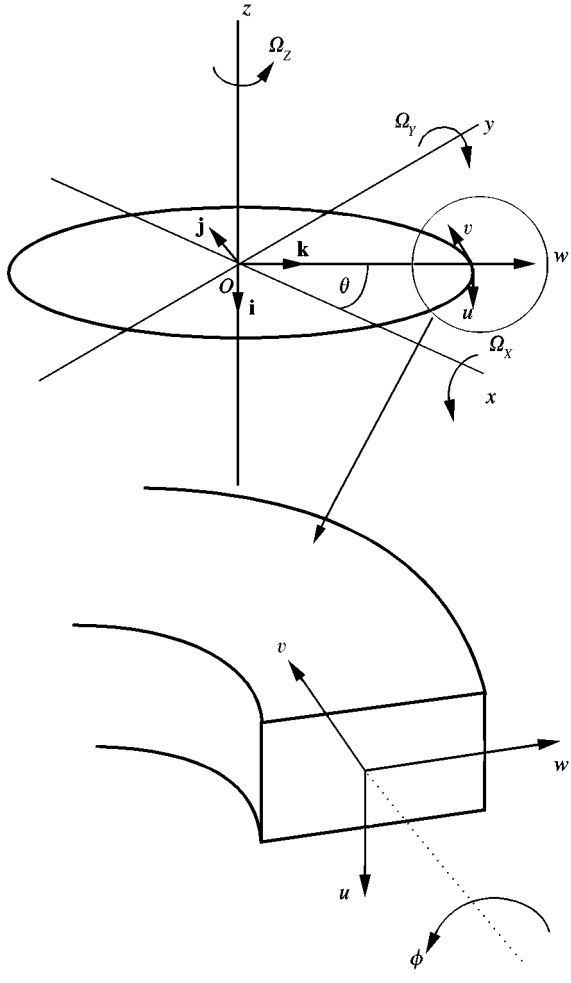

Figure 3. The ring model with enlarged view of displacements.

In-plane and out-of-plane elastic deformation of the ring is described in terms of four generalized co-ordinates Q_{I1}, Q_{I2}, Q_{O1}, Q_{O2}, which are based on the eigenvectors of a non-rotating circular ring, as will be described in the following section. The corresponding physical displacements of the ring comprise in-plane radial and tangential displacements, w and v, an out-of-plane translation, u and twisting, ϕ. Limiting the number of generalized co-ordinates to four is justified in the present analysis because the primary interest is in cases where the natural frequencies of the relevant in-plane and out-of-plane modes of the non-rotating ring are themselves closely spaced, but are well separated from the other modes. Under these conditions, the deflected shapes in free vibration will be dominated by the selected generalized coordinates. The kinetic and strain energies of the rotating ring can be expressed in terms of the generalized co-ordinates and then substituted into Lagrange's equation to obtain the equations of motion. The details are given in the following sections.

2.1. DISPLACEMENTS

The in-plane radial displacement, w, and tangential displacement, v, at an angular position, θ, can be expressed in terms of generalized co-ordinates $Q_{I1}(t)$ and $Q_{I2}(t)$ as [13]

$$\begin{Bmatrix} w \\ v \end{Bmatrix} = Q_{I1}(t) \begin{Bmatrix} n \sin n\theta \\ \cos n\theta \end{Bmatrix} + Q_{I2}(t) \begin{Bmatrix} n \cos n\theta \\ -\sin n\theta \end{Bmatrix}, \tag{1}$$

where the vectors associated with each generalized co-ordinate are taken as the eigenvectors for in-plane modes of vibration of a non-rotating inextensible circular ring for modes with n nodal diameters ($n = 2, 3, 4, \ldots$). Here, $\theta = 0$ coincides with Ox (see Figure 3).

The out-of-plane displacement of the ring section consists of a combination of translation, u, normal to the plane of the ring and twisting, ϕ, about the centroidal axis (see Figure 3). The out-of-plane displacements of the ring will be expressed in terms of generalized co-ordinates, $Q_{O1}(t)$ and $Q_{O2}(t)$ as [13]

$$\begin{Bmatrix} u \\ \phi \end{Bmatrix} = Q_{O1}(t) \begin{Bmatrix} 1 \\ -i^2\xi \end{Bmatrix} \cos i(\theta - \beta) + Q_{O2}(t) \begin{Bmatrix} -1 \\ i^2\xi \end{Bmatrix} \sin i(\theta - \beta), \tag{2}$$

where

$$\xi = \frac{1}{a}\left[\frac{1+\mu}{1+i^2\mu}\right], \quad \mu = \frac{GC_T}{EI_x} \quad \text{and} \quad C_T = \frac{cr_t^3 a_l^3}{r_t^2 + a_l^2}.$$

Again, the vectors associated with the generalized co-ordinates are taken as the eigenvectors of out-of-plane vibrations of an isotropic non-rotating inextensible circular ring for modes with i nodal diameters ($i = 2, 3, 4, \ldots$). In the above equations, a is the mean radius of the ring, r_t and a_l are the radial thickness and axial length of the ring respectively and c is a function of the ratio of r_t to a_l with values in the range 0·28–0·33 [13]. I_x is the second moment of area of the ring section and G and E are the shear and Young's moduli values for the material respectively.

The angle, β, in equation (2), accounts for a possible angular misalignment between the in-plane and out-of-plane generalized co-ordinates. For the ring to be used successfully as

a rate sensor, the angle, β, should ideally be zero to avoid unwanted coupling between the generalized co-ordinates. In practice, the ring would be trimmed to make $\beta = 0$. Therefore, to avoid unnecessary complexity whilst retaining the central features of the analysis, it will be assumed in the following analysis that $\beta = 0$.

2.2. ENERGY EXPRESSIONS

The kinetic energy of an element of the ring can be expressed as the sum of the contributions due to the velocity $\mathbf{v}_{abs}$, of the centroid of the cross-section and to the angular velocity of the element due to twisting $\dot{\phi}$ and to the applied rate components, Ω_X, Ω_Y, Ω_Z. It is convenient to express the linear and angular velocities in components along the local axial, tangential and radial directions, denoted by unit vectors **i**, **j**, **k** (see Figure 3). The summation over the entire ring can then be expressed as

$$T = \frac{1}{2}\rho A a \int_0^{2\pi} |\mathbf{v}_{abs}|^2 \, \mathrm{d}\theta + \frac{1}{2}\rho J a \int_0^{2\pi} |\dot{\boldsymbol{\phi}} + \mathbf{f}(\Omega_X, \Omega_Y)|^2 \, \mathrm{d}\theta, \tag{3}$$

where ρ, A and J define the density of the material, the cross-sectional area and the polar second moment of area of the ring section, $\dot{\boldsymbol{\phi}}$ can be expressed in terms of the generalized co-ordinates by using equation (2) and $\mathbf{f}(\Omega_X, \Omega_Y)$ represents the resolved components of applied rate about Ox and Oy. The absolute velocity of a general point on the ring at position $r(\theta)$ can be expressed as

$$\mathbf{v}_{abs} = \frac{\mathrm{d}\mathbf{r}}{\mathrm{d}t} + \boldsymbol{\Omega} \Lambda \mathbf{r} \tag{4}$$

where $\boldsymbol{\Omega}$ is the angular velocity of the local reference axes, given by

$$\boldsymbol{\Omega} = -\Omega_Z \mathbf{i} + (\Omega_Y \cos\theta - \Omega_X \sin\theta)\,\mathbf{j} + (\Omega_X \cos\theta + \Omega_Y \sin\theta)\mathbf{k}. \tag{5}$$

r can be described in terms of the displacements u, v and w in the local axial, tangential and radial directions (see Figure 3). By using equations (1) and (2) the position of the general point can then be expressed in terms of the generalized co-ordinates as follows:

$$\mathbf{r}(\theta) = (Q_{\mathrm{O}1} \cos i\theta - Q_{\mathrm{O}2} \sin i\theta)\mathbf{i} + (Q_{\mathrm{I}1} \cos n\theta + Q_{\mathrm{I}2} \sin n\theta)\mathbf{j}$$

$$+ (a + Q_{\mathrm{I}1} n \sin n\theta + Q_{\mathrm{I}2} n \cos n\theta)\mathbf{k}. \tag{6}$$

Substituting equations (5) and (6) into equation (4) gives the absolute velocity components in terms of several trigonometric functions and the generalized co-ordinates.

The kinetic energy, equation (3), can now be evaluated, and this leads to integrals whose magnitudes depend on the values of n and i and the relationship between them. Several terms have non-zero coefficients $n \pm 1 = i$ and are zero otherwise.

It is reasonable to neglect squares and products of Ω_X, Ω_Y, Ω_Z since, in practice, the applied angular velocities are much smaller ($x \sim 10^{-4}$) than the natural frequencies of the device and inertia forces due to centripetal acceleration are very small. For $n \geqslant 2$, the kinetic

energy can now be expressed as

$$T = \frac{1}{2}\rho A a \pi \left\{ \begin{array}{l} \dot{Q}_{I1}^2(n^2+1) + \dot{Q}_{I2}^2(n^2+1) + \dot{Q}_{O1}^2 + \dot{Q}_{O2}^2 \\ + 4\dot{Q}_{I1}Q_{I2}\Omega_Z n - 4\dot{Q}_{I2}Q_{I1}\Omega_Z n \\ + \dot{Q}_{I1}Q_{O1}\Omega_X(1 \mp n)_{\substack{n+1=i \\ n-1=i}} + \dot{Q}_{I1}Q_{O2}\Omega_Y(n \mp 1)_{\substack{n+1=i \\ n-1=i}} \\ + \dot{Q}_{I2}Q_{O1}\Omega_Y(-n \pm 1)_{\substack{n+1=i \\ n-1=i}} + \dot{Q}_{I2}Q_{O2}\Omega_X(1 \mp n)_{\substack{n+1=i \\ n-1=i}} \\ + \dot{Q}_{O1}Q_{I1}\Omega_X(-1 \pm n)_{\substack{n+1=i \\ n-1=i}} + \dot{Q}_{O1}Q_{I2}\Omega_Y(n \mp 1)_{\substack{n+1=i \\ n-1=i}} \\ + \dot{Q}_{O2}Q_{I1}\Omega_Y(-n \pm 1)_{\substack{n+1=i \\ n-1=i}} + \dot{Q}_{O2}Q_{I2}\Omega_X(-1 \pm n)_{\substack{n+1=i \\ n-1=i}} \end{array} \right\}$$

$$+ \frac{1}{2}\rho a J \pi i^4 \xi^2 \{\dot{Q}_{O1}^2 + \dot{Q}_{O2}^2\}. \tag{7}$$

The subscripts of the form $n + 1 = i$, etc., indicate the combinations of i and n for which the relevant term is non-zero.

The strain energy due to in-plane bending can be calculated as [14]

$$U_{IP} = \frac{EI_z}{2a^3}\int_0^{2\pi}\left[\frac{\partial^2 w}{\partial\theta^2} + w\right]^2 \mathrm{d}\theta = \frac{EI_z \pi n^2(n^2-1)^2}{2a^3}(Q_{I1}^2 + Q_{I2}^2) \tag{8}$$

where E and I_z are the Young's modulus of the material and the second moment of area about the centroidal axis normal to the plane of the ring. The radial displacement, w, is described in terms of the generalized co-ordinates, Q_{I1} and Q_{I2} by equation (1). The strain energy due to out-of-plane bending and twisting can be expressed as [15]

$$U_{OP} = \frac{EI_x}{2}\int_0^{2\pi} k_1^2 a\,\mathrm{d}\theta + \frac{C_T G}{2}\int_0^{2\pi} k_2^2 a\,\mathrm{d}\theta, \tag{9}$$

where

$$k_1 = \frac{1}{a}\left(\frac{1}{a}\frac{\partial^2 u}{\partial\theta^2} - \phi\right) \quad \text{and} \quad k_2 = \frac{1}{a}\left(\frac{\partial\phi}{\partial\theta} + \frac{1}{a}\frac{\partial u}{\partial\theta}\right). \tag{10}$$

Substituting for ϕ and u in equation (10) using equation (2) and evaluating the integrals of equation (9) gives

$$U_{OP} = \frac{i^2(i^2-1)^2\pi}{2a^3(1+i^2\mu)^2}[EI_x i^2\mu^2 + GC_T](Q_{O1}^2 + Q_{O2}^2). \tag{11}$$

Note that $n = 1$ and $i = 1$ correspond to rigid-body motion of an unsupported ring and the resulting zero strain energy is thus expected.

2.3. EQUATIONS OF MOTION

Substituting the energy expressions into Lagrange's equation [16] in the form

$$\frac{\mathrm{d}}{\mathrm{d}t}\left(\frac{\partial T}{\partial\dot{Q}_p}\right) - \frac{\partial T}{\partial Q_p} + \frac{\partial U}{\partial Q_p} = 0, \quad p = \mathrm{I1, I2, O1, O2}, \tag{12}$$

leads to the equations of motion for free, undamped vibration. Substituting equations (7), (8) and (11) into equation (12) gives, after a little algebra, the equations of motion in the form

$$[M]\{\ddot{q}\} + [G]\{\dot{q}\} + [K]\{q\} = \{0\}, \tag{13}$$

where

$$[M] = \begin{bmatrix} M_{\mathrm{I}}(1+\delta m_{\mathrm{I}1}) & 0 & 0 & 0 \\ 0 & M_{\mathrm{I}}(1+\delta m_{\mathrm{I}2}) & 0 & 0 \\ 0 & 0 & M_{\mathrm{O}}(1+\delta m_{\mathrm{O}1}) & 0 \\ 0 & 0 & 0 & M_{\mathrm{O}}(1+\delta m_{\mathrm{O}2}) \end{bmatrix}, \tag{14}$$

$$[G] = \rho A a \pi \times \begin{bmatrix} 0 & 4n\Omega_Z & \Omega_X(1 \mp n)_{\substack{n+1=i \\ n-1=i}} & \Omega_Y(n \mp 1)_{\substack{n+1=i \\ n-1=i}} \\ -4n\Omega_Z & 0 & -\Omega_Y(n \mp 1)_{\substack{n+1=i \\ n-1=i}} & \Omega_X(1 \mp n)_{\substack{n+1=i \\ n-1=i}} \\ -\Omega_X(1 \mp n)_{\substack{n+1=i \\ n-1=i}} & \Omega_Y(n \mp 1)_{\substack{n+1=i \\ n-1=i}} & 0 & 0 \\ -\Omega_Y(n \mp 1)_{\substack{n+1=i \\ n-1=i}} & -\Omega_X(1 \mp n)_{\substack{n+1=i \\ n-1=i}} & 0 & 0 \end{bmatrix}, \tag{15}$$

$$[K] = \begin{bmatrix} K_{\mathrm{I}}(1+\delta k_{\mathrm{I}1}) & 0 & 0 & 0 \\ 0 & K_{\mathrm{I}}(1+\delta k_{\mathrm{I}2}) & 0 & 0 \\ 0 & 0 & K_{\mathrm{O}}(1+\delta k_{\mathrm{O}1}) & 0 \\ 0 & 0 & 0 & K_{\mathrm{O}}(1+\delta k_{\mathrm{O}2}) \end{bmatrix}. \tag{16}$$

Here $R = [EI_x i^2 \mu^2 + GC_T]$, $M_{\mathrm{I}1}$, $M_{\mathrm{O}1}$, $K_{\mathrm{I}1}$, etc., are defined in Appendix A and

$$[q] = \{Q_{\mathrm{I}1}, Q_{\mathrm{I}2}, Q_{\mathrm{O}1}, Q_{\mathrm{O}2}\}^{\mathrm{T}}. \tag{17}$$

A number of points about the above equations require further comment at this stage. The mass and stiffness matrices, equations (14) and (16), contain the terms, $\delta m_{\mathrm{I}1}$, etc., and $\delta k_{\mathrm{I}1}$, etc., in addition to the terms which follow from the kinetic energy and strain energy expressions for the uniform ring, equations (7), (8) and (11). These additional (small) terms have been included to allow for the fact that, in practice, the ring may not be perfectly axi-symmetric. The effects of small departures from perfect circularity are quite complex and have been considered in detail in references [9–11]. For the present purposes, however, it is sufficient simply to note that imperfection would give rise to small additional terms in the mass and stiffness matrices whose practical effect would be to split the otherwise degenerate pairs of natural frequencies of the non-rotating ring. It has been assumed here that the imperfection is such that the off-diagonal terms in the mass and stiffness matrices are all zero. This is a special case, chosen for simplicity to illustrate the frequency-splitting effects without causing additional coupling between the generalized co-ordinates. The effect of any non-uniformity in the mass distribution on the gyroscopic coupling matrix $[G]$ has also been ignored. This is justified on the grounds that the input rates, Ω_X, Ω_Y, Ω_Z are small and therefore the effect on the predicted motion of any small changes to the gyroscopic coupling terms will be negligible.

When the rate input is zero, equation (13) uncouple into four separate equations of motion, one for each generalized co-ordinate. When rate is applied about all three axes, the presence of

terms in the gyroscopic coupling matrix, equation (15) shows the Coriolis coupling between various combinations of in-plane and out-of-plane generalized co-ordinates. It can be seen that rate applied about the polar axis, Ω_Z produces coupling between Q_{I1} and Q_{I2} for any value of n. This is the basis on which the existing single-axis rate sensor [1] operates. Applied rate about the polar axis does not couple in-plane and out-of-plane motions. However, angular velocity components, Ω_X and Ω_Y about axes in the plane of the ring do produce coupling between in-plane and out-of-plane motions, but only for particular combinations of i and n, given by $(n \pm 1 = i)$.

3. SOLUTIONS OF THE EQUATIONS OF MOTION

The principle of operation of a vibrating ring structure as a multi-axis rate sensor is described in reference [4], in which it is shown that it is desirable to select the dimensions of the ring so that the natural frequencies of the relevant modes of the non-rotating ring are equal. The natural frequencies and mode shapes for non-rotating inextensible rings are already well known [13] and ring dimensions can be chosen to match the required natural frequencies, if the ring is dimensionally perfect. In practice, small imperfections are inevitably present to some degree and these will give rise to small differences between the natural frequencies. It is therefore useful at this stage to assume that the natural frequencies of the non-rotating ring are distinct. These will be denoted by $\omega_{O1}, \omega_{O2}, \omega_{I1}, \omega_{I2}$ for the out-of-plane and in-plane modes respectively, as defined in Appendix A. For free undamped vibration, the solutions to equations (13) take the form

$$\{q\} = \{\bar{Q}\}\exp(j\omega t) \quad \text{where } \{\bar{Q}\}^T = \{\bar{Q}_{I1}, \bar{Q}_{I2}, \bar{Q}_{O1}, \bar{Q}_{O2}\} \tag{18}$$

and $\bar{Q}_{I1}$, etc., represent the complex amplitudes of the generalized co-ordinates. Substituting equation (18) into equation (13) and making use of equations (14)–(16), gives the characteristic equation for the system, after some algebraic manipulation, as

$$\omega^8 + C_6\omega^6 + C_4\omega^4 + C_2\omega^2 + C_0 = 0, \tag{19}$$

where

$$C_0 = \omega_{O1}^2\omega_{O2}^2\omega_{I1}^2\omega_{I2}^2, \tag{20}$$

$$C_2 = -[\omega_{O1}^2\omega_{O2}^2(\omega_{I1}^2 + \omega_{I2}^2) + \omega_{I1}^2\omega_{I2}^2(\omega_{O1}^2 + \omega_{O2}^2)] - \omega_{O1}^2\omega_{O2}^2\frac{G_Z^2\Omega_Z^2}{M_I^2}$$
$$- (\omega_{O1}^2\omega_{I1}^2 + \omega_{I2}^2\omega_{O2}^2)\frac{G_X^2\Omega_X^2}{M_O M_I} - (\omega_{O1}^2\omega_{I2}^2 + \omega_{I1}^2\omega_{O2}^2)\frac{G_Y^2\Omega_Y^2}{M_O M_I}, \tag{21}$$

$$C_4 = [\omega_{O1}^2\omega_{O2}^2 + (\omega_{O1}^2 + \omega_{O2}^2)(\omega_{I1}^2 + \omega_{I2}^2) + \omega_{I1}^2\omega_{I2}^2] + (\omega_{O1}^2 + \omega_{O2}^2)\frac{G_Z^2\Omega_Z^2}{M_I^2}$$
$$+ [\omega_{I1}^2 + \omega_{I2}^2 + \omega_{O1}^2 + \omega_{O2}^2]\frac{(G_X^2\Omega_X^2 + G_Y^2\Omega_Y^2)}{M_O M_I} + \frac{[G_X^2\Omega_X^2 + G_Y^2\Omega_Y^2]^2}{M_O^2 M_I^2}, \tag{22}$$

$$C_6 = -[\omega_{I1}^2 + \omega_{I2}^2 + \omega_{O1}^2 + \omega_{O2}^2] - \frac{G_Z^2\Omega_Z^2}{M_I^2} - \frac{2(G_X^2\Omega_X^2 + G_Y^2\Omega_Y^2)}{M_O M_I}. \tag{23}$$

It may be noted that those terms in the coefficients $C_O \ldots C_6$ given above which depend on the applied rates of turn, Ω_X, Ω_Y, Ω_Z, are much smaller in magnitude than the terms that are not associated with applied rate, because the analysis is based on the assumption that $\Omega \ll \omega$. The effects of the applied rate on the magnitudes of the natural frequencies will therefore be small, albeit important. For the general case where all the natural frequencies of the non-rotating ring are distinct and all the components of applied rate of turn are present, the natural frequencies can be found from equation (19), but the general effects of applied rate are not obvious. It is therefore useful to consider some more tractable, special cases to help provide some insight into the general behaviour.

3.1. RATE APPLIED ABOUT THE POLAR AXIS

For the case where $\Omega_X = 0 = \Omega_Y$, $\Omega_Z \neq 0$ the governing equations for out-of-plane motion, Q_{O1} and Q_{O2}, uncouple individually from the governing equations for in-plane motion, Q_{I1} and Q_{I2}, which remain coupled (see equations (13) and (15)). In this situation the coefficients of the characteristic equation (equations (20)–(23)) simplify considerably and equation (13) factorizes as

$$(\omega^2 - \omega_{O1}^2)(\omega^2 - \omega_{O2}^2)\left[\omega^4 - \omega^2\left(\omega_{I1}^2 + \omega_{I2}^2 + \frac{G_Z^2\Omega_Z^2}{M_I^2}\right) + \omega_{I1}^2\omega_{I2}^2\right] = 0. \tag{24}$$

The out-of-plane modes of the ring are unaffected by the applied rate in this case and their natural frequencies remain constant at ω_{O1}, ω_{O2}. Upon noting that $\Omega_Z \ll \omega_{I1}, \omega_{I2}$, the roots of the quadratic in the square bracket in equation (24) can be written with very good approximation as

$$\omega^2 \approx \frac{\omega_{I1}^2 + \omega_{I2}^2}{2}\left[1 \pm \sqrt{\frac{(\omega_{I1}^2 - \omega_{I2}^2)^2}{(\omega_{I1}^2 + \omega_{I2}^2)^2} + \frac{2G_Z^2\Omega_Z^2}{M_I^2(\omega_{I1}^2 + \omega_{I2}^2)}}\right]. \tag{25}$$

The amplitude ratios (mode shapes) corresponding to these natural frequencies follow in the usual way when equation (18) is substituted into equation (13) and can be written in the form

$$\frac{\bar{Q}_{I1}}{\bar{Q}_{I2}} = -\frac{jG_Z\Omega_Z\omega}{M_I(\omega_{I1}^2 - \omega^2)}. \tag{26}$$

Note that the mode shape expression, equation (26), is complex, indicating that the relative motions of the two generalized co-ordinates, Q_{I1} and Q_{I2}, are in quadrature.

If the ring is dimensionally perfect so that $\omega_{I1} = \omega_{I2} = \omega_I$ then it follows that the roots of equation (25) can be written as

$$\omega \approx \omega_I\left[1 + \frac{G_Z\Omega_Z}{2M_I\omega_I}\right] \quad \text{and} \quad \omega \approx \omega_I\left[1 - \frac{G_Z\Omega_Z}{2M_I\omega_I}\right], \tag{27}$$

equation (27) illustrates that, for small input rates, the initially equal frequencies of the in-plane modes split linearly with applied rate about the polar axis. However, if, due to dimensional imperfection, the initial split between ω_{I1} and ω_{I2} is significantly greater than the applied rate so that the first term under the square root in equation (25) dominates the second, then the applied rate has negligible effect on the natural frequencies which, from equation (25), are $\omega \approx \omega_{I1}$, $\omega \approx \omega_{I2}$. When the natural frequencies given by equation (27) are substituted

into equation (26) the corresponding amplitude ratios follow as

$$\frac{\bar{Q}_{I1}}{\bar{Q}_{I2}} \approx -\mathrm{j}\left[1 + \frac{G_Z\Omega_Z}{4M_I\omega_I}\right] \quad \text{and} \quad \frac{\bar{Q}_{I1}}{\bar{Q}_{I2}} \approx +\mathrm{j}\left[1 - \frac{G_Z\Omega_Z}{4M_I\omega_I}\right]. \tag{28}$$

Upon noting that $\Omega_Z/\omega_I \ll 1$, equation (28) can be further simplified and written as $\bar{Q}_{I1}/\bar{Q}_{I2} \approx \pm\mathrm{j}$. These points are illustrated more fully in section 4 of this paper.

3.2. RATE APPLIED ABOUT AXES IN THE PLANE OF THE RING

Consider the case where $\Omega_X \neq 0$ but $\Omega_Y = 0 = \Omega_Z$. In this case, substitution of the solutions, equation (18), into the equations of motion, equation (13), leads to the following set of equations for the amplitudes in which the motion of $\bar{Q}_{I1}$ and $\bar{Q}_{O1}$ is uncoupled from the motion of $\bar{Q}_{I2}$ and $\bar{Q}_{O2}$:

$$\begin{bmatrix} \omega_{I1}^2 - \omega^2 & \dfrac{\mathrm{j}\omega G_X\Omega_X}{M_I} & 0 & 0 \\ \dfrac{-\mathrm{j}\omega G_X\Omega_X}{M_O} & \omega_{O1}^2 - \omega^2 & 0 & 0 \\ 0 & 0 & \omega_{I2}^2 - \omega^2 & \dfrac{\mathrm{j}\omega G_X\Omega_X}{M_I} \\ 0 & 0 & \dfrac{-\mathrm{j}\omega G_X\Omega_X}{M_O} & \omega_{O2}^2 - \omega^2 \end{bmatrix} \begin{Bmatrix} \bar{Q}_{I1} \\ \bar{Q}_{O1} \\ \bar{Q}_{I2} \\ Q_{O2} \end{Bmatrix} = \begin{Bmatrix} 0 \\ 0 \\ 0 \\ 0 \end{Bmatrix}. \tag{29}$$

The frequency equation corresponding to generalized co-ordinates $\bar{Q}_{I1}$ and $\bar{Q}_{O1}$ follows from equation (29) as

$$\omega^4 - \omega^2\left(\omega_{I1}^2 + \omega_{O1}^2 + \frac{G_X^2\Omega_X^2}{M_OM_I}\right) + \omega_{I1}^2\omega_{O1}^2 = 0, \tag{30}$$

from which the natural frequencies can be expressed with good approximation as

$$\omega^2 \approx \frac{\omega_{I1}^2 + \omega_{O1}^2}{2}\left[1 \pm \sqrt{\frac{(\omega_{I1}^2 - \omega_{O1}^2)^2}{(\omega_{I1}^2 + \omega_{O1}^2)^2} + \frac{2G_X^2\Omega_X^2}{M_OM_I(\omega_{I1}^2 + \omega_{O1}^2)}}\right]. \tag{31}$$

The amplitude ratios, $\bar{Q}_{I1}/\bar{Q}_{O1}$, etc., can be determined from equation (29) and are of the form

$$\frac{\bar{Q}_{I1}}{\bar{Q}_{O1}} = -\frac{\mathrm{j}\omega G_X\Omega_X}{M_I(\omega_{I1}^2 - \omega^2)}. \tag{32}$$

If the dimensions of the ring are chosen such that the natural frequencies of the relevant in-plane and out-of-plane modes of the non-rotating ring are equal, i.e., $\omega_{I1} = \omega_{O1} = \omega_{OI}$ say, then the roots of equation (31) can be written as

$$\omega \approx \omega_{O1}\left[1 + \frac{G_X\Omega_X}{2\omega_{O1}\sqrt{M_OM_I}}\right] \quad \text{and} \quad \omega \approx \omega_{O1}\left[1 - \frac{G_X\Omega_X}{2\omega_{OI}\sqrt{M_OM_I}}\right]. \tag{33}$$

The amplitude ratios in this case can be found by using equations (32) and (33), and, upon noting that $\Omega_X/\omega_{OI} \ll 1$, the amplitude ratios can be expressed as

$$\frac{\bar{Q}_{I1}}{\bar{Q}_{O1}} = \frac{\bar{Q}_{I2}}{\bar{Q}_{O2}} \approx \pm\,\mathrm{j}\sqrt{\frac{M_O}{M_I}} = \pm\mathrm{j}\sqrt{\frac{1 + Ji^4\xi^2/A}{n^2 + 1}}, \tag{34}$$

where the $\pm$ signs correspond to those in equation (33). This simple result indicates that, under the conditions considered, the amplitude ratios are virtually independent of input rate and depend only on the effective modal masses of the relevant in-plane and out-of-plane modes of the non-rotating ring.

The natural frequencies and amplitude ratios for the system comprising generalized co-ordinates $\bar{Q}_{I2}$ and $\bar{Q}_{O2}$ can be obtained in a similar fashion.

The analysis for the case where rate is applied about the Oy axis only ($\Omega_Y \neq 0$ but $\Omega_X = 0 = \Omega_Z$) follows the same lines as shown above, but in that case the motion of $\bar{Q}_{I1}$ and $\bar{Q}_{O2}$ is uncoupled from the motion of $\bar{Q}_{I2}$ and $\bar{Q}_{O1}$. Corresponding expressions for the natural frequencies and mode shapes can be derived.

When rate is applied simultaneously about Ox and Oy ($\Omega_X \neq 0$, $\Omega_Y \neq 0$, $\Omega_Z = 0$), the analysis becomes more complicated because the generalized co-ordinates do not uncouple, and does not lead easily to simple expressions for the natural frequencies and amplitude ratios. However, in the particular case where $\omega_{I1} = \omega_{O1} = \omega_{I2} = \omega_{O2} = \omega_{OI}$ (i.e., dimensionally perfect ring with dimensions chosen such that the natural frequencies of the relevant in-plane and out-of-plane modes of the non-rotating ring are equal), the coefficients of the characteristic equation, equation (19), simplify considerably to the following:

$$C_0 = \omega_{OI}^8, \tag{35}$$

$$C_2 = -4\omega_{OI}^6 - 2\omega_{OI}^4 \frac{G_X^2\Omega_X^2 + G_Y^2\Omega_Y^2}{M_O M_I}, \tag{36}$$

$$C_4 = 6\omega_{OI}^4 + 4\omega_{OI}^2 \frac{(G_X^2\Omega_X^2 + G_Y^2\Omega_Y^2)}{M_O M_I} + \frac{[G_X^2\Omega_X^2 + G_Y^2\Omega_Y^2]^2}{M_O^2 M_I^2}, \tag{37}$$

$$C_6 = -4\omega_{OI}^2 - \frac{2(G_X^2\Omega_X^2 + G_Y^2\Omega_Y^2)}{M_O M_I}, \tag{38}$$

and the characteristic equation factorizes as

$$\left[(\omega^2 - \omega_{OI}^2)^2 - \omega^2 \frac{(G_X^2\Omega_X^2 + G_Y^2\Omega_Y^2)}{M_O M_I}\right]^2 = 0. \tag{39}$$

The repeated roots of equation (39) can be written with good approximation as

$$\omega \approx \omega_{OI}\left[1 + \frac{\sqrt{G_X^2\Omega_X^2 + G_Y^2\Omega_Y^2}}{2\omega_{OI}\sqrt{M_O M_I}}\right] \quad \text{and} \quad \omega \approx \omega_{OI}\left[1 - \frac{\sqrt{G_X^2\Omega_X^2 + G_Y^2\Omega_Y^2}}{2\omega_{O1}\sqrt{M_O M_I}}\right]. \tag{40}$$

Upon noting that $G_X^2 = G_Y^2$, a comparison of equations (40) and (33) shows that, for the special case under consideration, the effect on the natural frequencies of a particular resultant value of externally applied rate is independent of the axis about which the rate is applied. This is consistent with intuition because the circumferential position of the modes is arbitrary if the ring is perfect.

3.3. RATE APPLIED SIMULTANEOUSLY ABOUT AN IN-PLANE AXIS AND THE POLAR AXIS

Consider the special case where $\omega_{I1} = \omega_{O1} = \omega_{I2} = \omega_{O2} = \omega_{O1}$ and the input rates are applied such that $\Omega_X \neq 0$, $\Omega_Y = 0$, $\Omega_Z \neq 0$. For this situation, the coefficients of the

characteristic equation, equations (19)–(23), simplify so that the characteristic equation, equation (19), can be factorized in the following form:

$$\left[(\omega^2-\omega_{\mathrm{OI}}^2)^2-\omega^2\frac{G_X^2\Omega_X^2}{M_{\mathrm{O}}M_{\mathrm{I}}}+(\omega^2-\omega_{\mathrm{OI}}^2)\omega\frac{G_Z\Omega_Z}{M_{\mathrm{I}}}\right]$$
$$\times\left[(\omega^2-\omega_{\mathrm{OI}}^2)^2-\omega^2\frac{G_X^2\Omega_X^2}{M_{\mathrm{O}}M_{\mathrm{I}}}-(\omega^2-\omega_{\mathrm{OI}}^2)\omega\frac{G_Z\Omega_Z}{M_{\mathrm{I}}}\right]=0. \tag{41}$$

Each of the expressions in square brackets in equation (41) leads to two positive values of ω^2 that are roots of the characteristic equation. It can be seen that when $\Omega_X=0$, $\Omega_Z=0$, equation (41) has four equal roots, ω_{OI}. Upon noting that Ω_X, $\Omega_Z \ll \omega_{\mathrm{OI}}$, it is clear that when $\Omega_X\neq 0$, $\Omega_Z\neq 0$ the roots of equation (41) will differ only slightly from ω_{OI}, which is confirmed by numerical evaluation of the roots. This fact makes it possible to construct a perturbation solution for the roots of equation (41) as follows.

The bracketed terms in equation (41) can be expanded and written as

$$\omega^4\mp\frac{G_Z\Omega_Z}{M_{\mathrm{I}}}\omega^3-\left(2\omega_{\mathrm{OI}}^2+\frac{G_X^2\Omega_X^2}{M_{\mathrm{O}}M_{\mathrm{I}}}\right)\omega^2\pm\omega_{\mathrm{OI}}^2\frac{G_Z\Omega_Z}{M_{\mathrm{I}}}\omega+\omega_{\mathrm{OI}}^4=0. \tag{42}$$

Upon noting that the roots of equation (42) are close to ω_{OI}, they can be expressed as

$$\omega=\omega_{\mathrm{OI}}(1+\varepsilon), \tag{43}$$

where ε is a small parameter of order $O(\Omega_{X,Z}/\omega_{\mathrm{OI}})$. Substituting equation (43) into each of the two forms of equation (42) and retaining terms up to those of order $O(\varepsilon^2)$ leads to two quadratics which provide four distinct values of ε as follows:

$$\varepsilon_{1,3}=-\frac{G_Z\Omega_Z}{4\omega_{\mathrm{OI}}M_{\mathrm{I}}}\mp\frac{1}{4\omega_{\mathrm{OI}}M_{\mathrm{I}}}\sqrt{G_Z^2\Omega_Z^2+4\frac{M_{\mathrm{I}}}{M_{\mathrm{O}}}G_X^2\Omega_X^2},$$
$$\varepsilon_{2,4}=+\frac{G_Z\Omega_Z}{4\omega_{\mathrm{OI}}M_{\mathrm{I}}}\mp\frac{1}{4\omega_{\mathrm{OI}}M_{\mathrm{I}}}\sqrt{G_Z^2\Omega_Z^2+4\frac{M_{\mathrm{I}}}{M_{\mathrm{O}}}G_X^2\Omega_X^2}. \tag{44}$$

Equations (43) and (44) provide simple, accurate approximations for the natural frequencies of the rotating ring under the condition where rate is simultaneously applied about an in-plane axis and the polar axis. In the case where either $\Omega_X=0$ or $\Omega_Z=0$ the above approximations simplify as expected to give equation (27) or (33).

The ratios of the amplitudes of the generalized co-ordinates which define the mode shapes corresponding to each of the natural frequencies can be found routinely by back-substitution using equations (18) and (13), but the resulting expressions do not lend themselves to useful simplification. A numerical example of this case is presented in section 4.1.3.

4. NUMERICAL EXAMPLES

It is desirable to quantify the effects that applied rates will have on the natural frequencies and mode shapes of the ring structure. This will be done by means of numerical examples based on a ring of nickel/steel alloy (Young's modulus and shear modulus values are 170×10^9

and 653×10^8 Pa respectively and the density is 8250 kg/m^3) with mean radius 20 mm and radial thickness 1 mm. The axial thickness of the ring is selected to match the natural frequency of the $n = 4$ in-plane modes to either the $i = 3$ or the $i = 5$ out-of-plane modes for the non-rotating ring. These values apply to a prototype multi-axis rate sensor. Initially, we will consider the ideal case in which all the relevant natural frequencies are matched $\sim$7·5 kHz. In practice, due to manufacturing tolerances there is likely to be a frequency split between mode frequencies and some specific cases of this will be investigated. We consider a range of constant rate inputs in the range 0–10 Hz applied about each axis individually.

4.1. EQUAL NON-ROTATING NATURAL FREQUENCIES

Consider the case where the axial length is chosen to match the frequencies of the $n = 4$ in-plane modes to either the $i = 3$ or the $i = 5$ out-of-plane modes at a frequency of $\sim$7587 Hz in the non-rotating ring, which is perfectly axi-symmetric (i.e., $\omega_{I1} = \omega_{I2} = \omega_{O1} = \omega_{O2}$).

4.1.1. *Rate applied about the polar axis*

For rates $\Omega_z = 1, 5, 10$ Hz applied about the polar axis, equation (24) gives values for the four natural frequencies ($\omega_{1Z}, \omega_{2Z}, \omega_{3Z}, \omega_{4Z}$) of the rotating ring as shown in Table 1. Figure 4 shows the variations of ω_{1Z} and ω_{2Z}. When no rate is applied the natural frequencies of the ring are identical, as expected. As the rate is increased, ω_{1Z} increases whilst ω_{2Z} decreases. Both values show a sensibly linear variation with applied rate for the range of Ω_z considered, in agreement with the approximate solution of the frequency equation as given in equation (27). The frequency split is symmetrical about the natural frequency for the non-rotating ring and increases to give a split of $\sim$9 Hz at an applied rate of 10 Hz which is $\sim$0·12% of the mean value.

The corresponding amplitude ratios, $\bar{Q}_{I1}/\bar{Q}_{I2}$, for the rotating ring can be found by using equation (26) or (28). For the range of values of Ω_z considered here, the magnitude of the amplitude ratio is equal to unity to four significant figures.

4.1.2. *Rate applied about an in-plane axis*

Consider rates $\Omega_x = 1, 5, 10$ Hz applied about the in-plane Ox axis. (Note that the same rates of turn applied about any axis in the plane of the ring would lead to the same patterns of behaviour as predicted for the cases considered below.) For the ideal case where $\omega_{I1} = \omega_{I2} = \omega_{O1} = \omega_{O2} = \omega_{OI}$ the (repeated) natural frequencies of the rotating ring are given

TABLE 1

Natural frequencies when rate is applied about the polar axis, Oz, when n = 4 and i = 3 or 5

Ω_z (Hz)	ω_{1Z} (Hz)	ω_{2Z} (Hz)	$\omega_{3Z} = \omega_{4Z}$ (Hz)
0	7587·4	7587·4	7587·4
1	7587·9	7586·9	7587·4
5	7589·8	7585·1	7587·4
10	7592·1	7582·7	7587·4

Note: These results apply for the case where $\omega_{I1} = \omega_{I2} = \omega_{O1} = \omega_{O2}$.

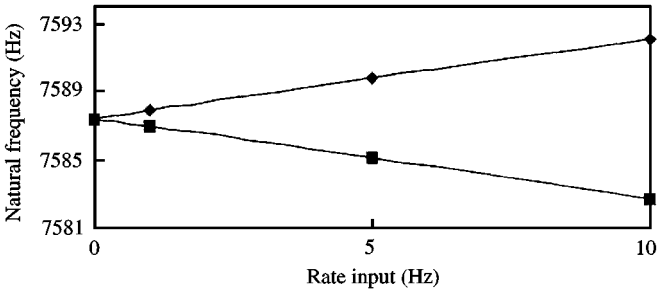

Figure 4. Natural frequency variations with rate applied about the polar axis, Oz ($n = 4$; —◆—. ω_{1Z}; —■—, ω_{2Z}).

TABLE 2

Natural frequencies and amplitude ratios for rates applied about the in-plane Ox axis when $n = 4$ and $i = 5$

Ω_x (Hz)	$\omega_{1X} = \omega_{3X}$ (Hz)	$\dfrac{\bar{Q}_{I1}}{\bar{Q}_{O1}} = -\dfrac{\bar{Q}_{I2}}{\bar{Q}_{O2}}$	$\omega_{2X} = \omega_{4X}$ (Hz)	$\dfrac{\bar{Q}_{I1}}{\bar{Q}_{O1}} = -\dfrac{\bar{Q}_{I2}}{\bar{Q}_{O2}}$
0	7587·4		7587·4	
1	7587·7	−j0·2634 ($\omega_{1X} = \omega_{3X}$)	7587·1	j0·2634 ($\omega_{2X} = \omega_{4X}$)
5	7589·1	−j0·2634 ($\omega_{1X} = \omega_{3X}$)	7585·7	j0·2634 ($\omega_{2X} = \omega_{4X}$)
10	7590·8	− j0·2634 ($\omega_{1X} = \omega_{3X}$)	7584·1	j0·2634 ($\omega_{2X} = \omega_{4X}$)

Notes: These results apply for the case where $\omega_{I1} = \omega_{I2} = \omega_{O1} = \omega_{O2}$ (for $n = 4$, $i = 5$).
Bracketed symbols indicate which solution for the natural frequency is substituted into equation (27). Amplitude ratios are given to 4 significant figures.

by the roots of equation (30), which can be written with good approximation as shown by equation (34).

Consider first the case where the axial thickness ($\sim$0·617 mm) is chosen to match the $n = 4$ in-plane frequencies to the $i = 5$ out-of-plane mode frequencies for the non-rotating ring. For this case, the natural frequencies of the rotating ring are shown in Table 2. The variation in the natural frequencies, for Ω_x in the range 0–10 Hz, is shown graphically in Figure 5. When no rate is applied about the Ox axis, all natural frequency values are equal to the natural frequency of the non-rotating ring, as expected. When rate is applied, $\omega_{1X}(=\omega_{3X})$ increases whilst $\omega_{2X}(=\omega_{4X})$ decreases. As predicted, both values show a sensibly linear variation with increasing applied rate for Ω_x in the range considered. The split between the frequencies is symmetrical about the natural frequency for the non-rotating ring and increases to give a frequency split of $\sim$6·7 Hz at an applied rate of 10 Hz which is $\sim$0·09% of the mean value.

The amplitude ratios for the rotating ring, calculated by using equation (32) are shown in Table 2 as the ratio of $\bar{Q}_{I1}/\bar{Q}_{O1}(= -\bar{Q}_{I2}/\bar{Q}_{O2})$ for $\Omega_x = 1$, 5, 10 Hz. These are equal in magnitude and opposite in sign depending on whether $\omega_{1X}(=\omega_{3X})$ or $\omega_{2X}(=\omega_{4X})$ is used, and are independent of Ω_x to seven significant figures. This is consistent with the expressions given in equation (34), which provide excellent simple approximations for the amplitude ratios for low values of rate input.

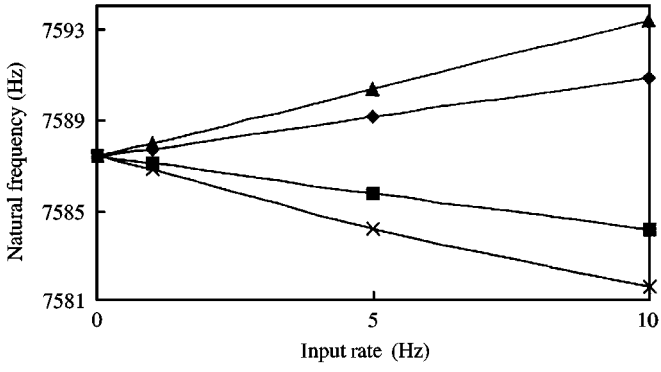

Figure 5. Natural frequency variations with rate applied about the in-plane Ox axis when $\omega_{I1} = \omega_{I2} = \omega_{O1} = \omega_{O2}$. [$n = 4$: —◆—, $\omega_{1X} = \omega_{3X}$ ($i = 5$); —■—, $\omega_{2X} = \omega_{4X}$ ($i = 5$); —▲—, $\omega_{1X} = \omega_{3X}$ ($i = 3$); —×—, $\omega_{2X} = \omega_{4X}$ ($i = 3$)].

TABLE 3

Natural frequencies and amplitude ratios for rates applied about the in-plane Ox axis when $n = 4$ and $i = 3$

Ω_x (Hz)	$\omega_{1X} = \omega_{3X}$ (Hz)	$\dfrac{\bar{Q}_{I1}}{\bar{Q}_{O1}} = -\dfrac{\bar{Q}_{I2}}{\bar{Q}_{O2}}$	$\omega_{2X} = \omega_{4X}$ (Hz)	$\dfrac{\bar{Q}_{I1}}{\bar{Q}_{O1}} = -\dfrac{\bar{Q}_{I2}}{\bar{Q}_{O2}}$
0	7587·4		7587·4	
1	7588·0	j0·2538 ($\omega_{1X} = \omega_{3X}$)	7586·8	− j0·2538 ($\omega_{2X} = \omega_{4X}$)
5	7590·3	j0·2538 ($\omega_{1X} = \omega_{3X}$)	7584·2	− j0·2538 ($\omega_{2X} = \omega_{4X}$)
10	7593·2	j0·2538 ($\omega_{1X} = \omega_{3X}$)	7581·6	− j0·2538 ($\omega_{2X} = \omega_{4X}$)

Notes: These results apply for the case where $\omega_{I1} = \omega_{I2} = \omega_{O1} = \omega_{O2}$ (for $i = 3$). Bracketed symbols indicate which solution for the natural frequency is substituted into equation (27). Amplitude ratios are given to 4 significant figures.

Consider now the case where an axial thickness ($\sim 2{\cdot}159$ mm) is chosen to match the $n = 4$ in-plane mode frequency and the $i = 3$ out-of-plane mode frequency for the non-rotating ring. For this case the corresponding natural frequencies and amplitude ratios of the rotating ring are shown in Table 3. The variations in natural frequencies are shown in Figure 5 (along with the values for the case where $i = 5$). The general pattern of behaviour for $i = 3$ is seen to be the same as for $i = 5$, but the frequency splitting is slightly greater because the different value of i, and the different dimensions of the ring cross-section, give rise to a different value of M_O. The frequency split is again symmetrical about the natural frequency for the non-rotating ring and at an applied rate of 10 Hz the split increases to $\sim 11{\cdot}6$ Hz which is $\sim 0{\cdot}15\%$ of the mean value. The amplitude ratios for the case $i = 3$ follow a similar pattern to the previously discussed case where $i = 5$.

4.1.3. *Rate applied about an in-plane axis and the polar axis simultaneously*

Results are presented for the case where rates in the range $\Omega_X = \Omega_Z = 1, 5, 10$ Hz are applied about the Ox and Oz axes simultaneously with $\Omega_Y = 0$. As before, we consider

TABLE 4

Natural frequencies for rates applied simultaneously about the in-plane Ox axis and the polar axis, Oz, when $n = 4$ and $i = 3$

$\Omega_x = \Omega_z$ (Hz)	ω_{1XZ} (Hz)	ω_{2XZ} (Hz)	ω_{3XZ} (Hz)	ω_{4XZ} (Hz)
0	7587·4	7587·4	7587·4	7587.4
1	7587·8	7587·0	7588·3	7586·5
5	7589·5	7585·4	7591·8	7583·0
10	7591·5	7583·3	7596·2	7578·6

Note: These results apply for the case where $\omega_{I1} = \omega_{I2} = \omega_{O1} = \omega_{O2}$ (for $n = 4$, $i = 3$).

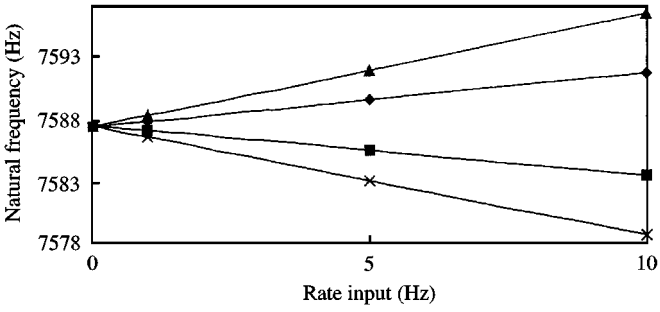

Figure 6. Natural frequency variations with equal rates applied about the in-plane Ox axis and the polar axis Oz when $\omega_{I1} = \omega_{I2} = \omega_{O1} = \omega_{O2}$. [$n = 4$, $i = 3$: —◆—, ω_{1XZ}; —■—, ω_{2XZ}; —▲—, ω_{3XZ}; —×—, ω_{4XZ}].

a perfectly axi-symmetric ring with dimensions chosen to match frequencies of the $n = 4$ in-plane mode and the $i = 3$ out-of-plane mode of the non-rotating ring. The relevant natural frequencies (ω_{1XZ}, ω_{2XZ}, ω_{3XZ}, ω_{4XZ}) of the rotating ring are found by using equation (41). They are given in Table 4 and illustrated graphically in Figure 6 which, as in the other cases, shows a sensibly linear variation in the natural frequencies as the applied rate increases with percentage frequency splits of the same order as when the rate components are applied individually. The corresponding amplitude ratios are given in Table 5. Finally, Tables 6 and 7 present natural frequency and amplitude ratio results for the case where dimensions are chosen to match frequencies of the $n = 4$ and $i = 5$ modes on the non-rotating ring.

In the above cases, the simultaneous presence of applied rate about in-plane and polar axes causes frequency splitting between all four relevant natural frequencies and the motions of all four generalized co-ordinates are coupled. It can be seen from Tables 5 and 7 that, under the considered conditions, the relative amplitudes of $\bar{Q}_{I1}$ and $\bar{Q}_{I2}$ are the same (to within more than four significant figures), as are the relative amplitudes of $\bar{Q}_{O1}$ and $\bar{Q}_{O2}$, and that the ratios of those magnitudes are constant. This is consistent with the observed behaviour when the rate is applied individually about either the polar axis or about an in-plane axis. The fact that the relative amplitudes of $\bar{Q}_{O1}$ and $\bar{Q}_{O2}$ are greater than those of $\bar{Q}_{I1}$ and $\bar{Q}_{I2}$ in the examples chosen has no particular significance and depends on a number of factors including the relative magnitudes of the rate components, Ω_X and Ω_Z, and the values of the coefficients G_X, G_Z and M_O, M_I.

TABLE 5

Amplitude ratios when rate is applied about the in-plane Ox axis and the polar axis, Oz simultaneously when $n = 4$ and $i = 3$

	$\Omega_x = \Omega_z = 1$ (Hz)		$\Omega_x = \Omega_z = 5$ (Hz)		$\Omega_x = \Omega_z = 10$ (Hz)	
$\bar{Q}_{I1}$	1	1	1	1	1	1
$\bar{Q}_{I2}$	$\pm j_{\substack{\omega_{1XZ} \\ \omega_{2XZ}}}$	$\mp j_{\substack{\omega_{3XZ} \\ \omega_{4XZ}}}$	$\pm j_{\substack{\omega_{1XZ} \\ \omega_{2XZ}}}$	$\mp j_{\substack{\omega_{3XZ} \\ \omega_{4XZ}}}$	$\pm j_{\substack{\omega_{1XZ} \\ \omega_{2XZ}}}$	$\mp j_{\substack{\omega_{3XZ} \\ \omega_{4XZ}}}$
$\bar{Q}_{O1}$	$\mp j\ 5{\cdot}998_{\substack{\omega_{1XZ} \\ \omega_{2XZ}}}$	$\mp j2{\cdot}980_{\substack{\omega_{3XZ} \\ \omega_{4XZ}}}$	$\mp j5{\cdot}998_{\substack{\omega_{1XZ} \\ \omega_{2XZ}}}$	$\mp j2{\cdot}980_{\substack{\omega_{3XZ} \\ \omega_{4XZ}}}$	$\mp j5{\cdot}998_{\substack{\omega_{1XZ} \\ \omega_{2XZ}}}$	$\mp j2{\cdot}980_{\substack{\omega_{3XZ} \\ \omega_{4XZ}}}$
$\bar{Q}_{O2}$	$5{\cdot}998_{\substack{\omega_{1XZ} \\ \omega_{2XZ}}}$	$-2{\cdot}980_{\substack{\omega_{3XZ} \\ \omega_{4XZ}}}$	$5{\cdot}998_{\substack{\omega_{1XZ} \\ \omega_{2XZ}}}$	$-2{\cdot}980_{\substack{\omega_{3XZ} \\ \omega_{4XZ}}}$	$5{\cdot}998_{\substack{\omega_{1XZ} \\ \omega_{2XZ}}}$	$-2{\cdot}980_{\substack{\omega_{3XZ} \\ \omega_{4XZ}}}$

Notes: These results apply for the case where $\omega_{I1} = \omega_{I2} = \omega_{O1} = \omega_{O2}$ (for $i = 3$, $n = 4$). The subscripts denote which frequency value from Table 4 is substituted into the amplitude ratio equation. Amplitude ratios are given to four significant figures. The subscripts relate to the corresponding element of the $\pm$sign, where one is shown.

TABLE 6

Natural frequencies when rate is applied simultaneously about the in-plane Ox axis and the polar axis, Oz when $n = 4$ and $i = 5$

$\Omega_x = \Omega_z$ (Hz)	ω_{1XZ} (Hz)	ω_{2XZ} (Hz)	ω_{3XZ} (Hz)	ω_{4XZ} (Hz)
0	7587·4	7587·4	7587·4	7587.4
1	7587·6	7587·2	7588·1	7586·7
5	7588·4	7586·4	7590·8	7584·1
10	7589·4	7585·4	7594·1	7580·7

Notes: These results apply for the case where $\omega_{I1} = \omega_{I2} = \omega_{O1} = \omega_{O2}$ (for $n = 4$, $i = 5$).

TABLE 7

Amplitude ratios when rate is applied simultaneously about the in-plane Ox axis and the polar axis, Oz when $n = 4$ and $i = 5$

	$\Omega_x = \Omega_z = 1$ (Hz)		$\Omega_x = \Omega_z = 5$ (Hz)		$\Omega_x = \Omega_z = 10$ (Hz)	
$\bar{Q}_{I1}$	1	1	1	1	1	1
$\bar{Q}_{I2}$	$\pm j_{\substack{\omega_{1XZ} \\ \omega_{2XZ}}}$	$\mp j_{\substack{\omega_{3XZ} \\ \omega_{4XZ}}}$	$\pm j_{\substack{\omega_{1XZ} \\ \omega_{2XZ}}}$	$\mp j_{\substack{\omega_{3XZ} \\ \omega_{4XZ}}}$	$\pm j_{\substack{\omega_{1XZ} \\ \omega_{2XZ}}}$	$\mp j_{\substack{\omega_{3XZ} \\ \omega_{4XZ}}}$
$\bar{Q}_{O1}$	$\pm j7{\cdot}575_{\substack{\omega_{1XZ} \\ \omega_{2XZ}}}$	$\pm j2{\cdot}242_{\substack{\omega_{3XZ} \\ \omega_{4XZ}}}$	$\pm j7{\cdot}575_{\substack{\omega_{1XZ} \\ \omega_{2XZ}}}$	$\pm j2{\cdot}242_{\substack{\omega_{3XZ} \\ \omega_{4XZ}}}$	$\pm j7{\cdot}575_{\substack{\omega_{1XZ} \\ \omega_{2XZ}}}$	$\pm j2{\cdot}242_{\substack{\omega_{3XZ} \\ \omega_{4XZ}}}$
$\bar{Q}_{O2}$	$-7{\cdot}575_{\substack{\omega_{1XZ} \\ \omega_{2XZ}}}$	$2{\cdot}242_{\substack{\omega_{3XZ} \\ \omega_{4XZ}}}$	$-7{\cdot}575_{\substack{\omega_{1XZ} \\ \omega_{2XZ}}}$	$2{\cdot}242_{\substack{\omega_{3XZ} \\ \omega_{4XZ}}}$	$-7{\cdot}575_{\substack{\omega_{1XZ} \\ \omega_{2XZ}}}$	$2{\cdot}242_{\substack{\omega_{3XZ} \\ \omega_{4XZ}}}$

Notes: For the case where $\omega_{I1} = \omega_{I2} = \omega_{O1} = \omega_{O2}$ (for $i = 5$, $n = 4$). The subscripts denote which frequency value from Table 6 is substituted into the amplitude ratio equation. Amplitude ratios are given to four significant figures. The subscripts relate to the corresponding element of the $\pm$sign, where one is shown.

TABLE 8

Natural frequencies when rate is applied about the polar axis when there is a 1 Hz split between the $n = 4$ and $i = 3$ modes of the non-rotating ring

Ω_z (Hz)	ω_{1Z} (Hz)	ω_{2Z} (Hz)	$\omega_{3Z} = \omega_{4Z}$ (Hz)
0	7587·4	7587·4	7588·4
1	7587·9	7586·9	7588·4
5	7589·8	7585·1	7588·4
10	7592·1	7582·7	7588·4

Notes: These results apply for the case where $\omega_{I1} = \omega_{I2} = \omega_I$ ($n = 4$) and $\omega_{O1} = \omega_{O2} = \omega_O$ ($i = 3$) and $\omega_O = \omega_I + 1$ (Hz).

4.2. INITIAL FREQUENCY SPLIT BETWEEN IN-PLANE AND OUT-OF-PLANE MODES

Due to manufacturing tolerances and other imperfections there may be a split between mode frequencies. To illustrate the effect of this, consider the case where, in the non-rotating ring, the natural frequencies of the relevant pair of in-plane modes are equal ($\omega_{I1} = \omega_{I2} = \omega_I$), and the frequencies of the relevant pair of out-of-plane modes are also equal ($\omega_{O1} = \omega_{O2} = \omega_O$), but $\omega_I \neq \omega_O$. We consider a 1 Hz (0·01%) split between the in-plane pair and out-of-plane pair of modes (i.e. $\omega_I \sim 7587$ Hz and $\omega_O \sim 7588$ Hz), which is a practically relevant example.

4.2.1. *Rate applied about the polar axis*

Consider applied rates $\Omega_z = 1, 5, 10$ Hz as before. The relevant characteristic equation for this case is equation (24) with $\omega_{I1} = \omega_{I2} = \omega_I$ and $\omega_{O1} = \omega_{O2} = \omega_O$. It can be seen from equation (24) that the out-of-plane modes are independent of the applied rate but the frequencies of the in-plane modes are split by the applied rate. The natural frequencies are shown in Table 8 and the amplitude ratios corresponding to ω_{1Z} and ω_{2Z} are essentially $\pm$j as given by equation (28).

4.2.2. *Rate applied about an in-plane axis*

The natural frequencies and amplitude ratios for this case are given with good approximation by equations (31) and (32) with $\omega_{I1} = \omega_{I2} = \omega_I$ and $\omega_{O1} = \omega_{O2} = \omega_O$. Because the ring is axi-symmetric, the natural frequencies are repeated.

In a similar fashion to section 4.1.2, we will consider the two cases where the $n = 4$ inplane frequencies are close to the $i = 5$ and $i = 3$ out-of-plane frequencies respectively, for the non-rotating ring. An initial 1 Hz split between the in-plane and out-of-plane mode frequencies will be assumed. We will consider a rate input applied about axis Ox, but the general behaviour will be the same for rates applied about any other in-plane axis.

For the case $n = 4$, $i = 5$ the natural frequencies and amplitude ratios for $\Omega_x = 1, 5, 10$ Hz are shown in Table 9. When no rate is applied there is a 1 Hz split between the natural frequency values as expected from equation (31). The variations in natural frequency with increasing Ω_x are shown graphically in Figure 7. As Ω_x increases, $\omega_{1X} (= \omega_{3X})$ increases whilst $\omega_{2X} (= \omega_{4X})$ decreases. At an applied rate of 1 Hz the split between the frequencies is $\sim$1·2 Hz. This value is 80% greater than when all the natural frequencies are initially matched (see

TABLE 9

Natural frequencies and amplitude ratios for rates applied about the in-plane Ox axis when there is a 1 Hz split between the $n = 4$ and $i = 5$ modes of the non-rotating ring

Ω_x (Hz)	$\omega_{1X} = \omega_{3X}$ (Hz)	$\dfrac{\bar{Q}_{I1}}{\bar{Q}_{O1}} = -\dfrac{\bar{Q}_{I2}}{\bar{Q}_{O2}}$	$\omega_{2X} = \omega_{4X}$ (Hz)	$\dfrac{\bar{Q}_{I1}}{\bar{Q}_{O1}} = -\dfrac{\bar{Q}_{I2}}{\bar{Q}_{O2}}$
0	7588·4		7587·4	
1	7588·5	−j0·08009 ($\omega_{1X} = \omega_{3X}$)	7587·3	j0·8667 ($\omega_{2X} = \omega_{4X}$)
5	7589·7	−j0·1963 ($\omega_{1X} = \omega_{3X}$)	7586·2	j0·3536 ($\omega_{2X} = \omega_{4X}$)
10	7591·3	− j0·2270 ($\omega_{1X} = \omega_{3X}$)	7584·5	j0·3057 ($\omega_{2X} = \omega_{4X}$)

Notes: These results apply for the case where $\omega_{I1} = \omega_{I2} = \omega_I$ and $\omega_{O1} = \omega_{O2} = \omega_O$ and $\omega_O = \omega_I + 1$ (for $i = 5$). Bracketed symbols indicate which solution for the natural frequency is substituted into equation (27). Amplitude ratios are given to four significant figures.

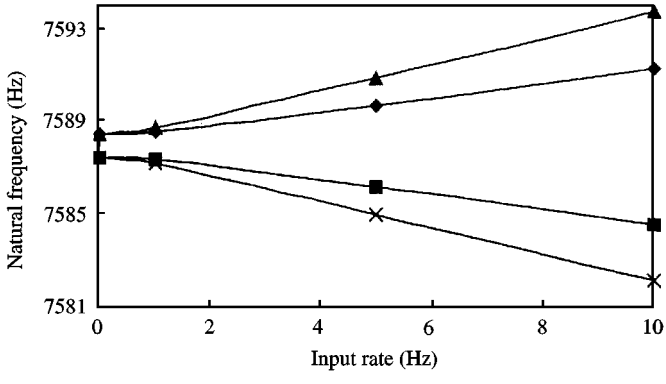

Figure 7. Natural frequency variations with equal rates applied about the in-plane Ox axis when $\omega_{I1} = \omega_{I2} = \omega_I$ and $\omega_{O1} = \omega_{O2} = \omega_O$. [$n = 4$: —◆—, $\omega_{1X} = \omega_{3X}$ ($i = 5$); —■—, $\omega_{2X} = \omega_{4X}$ ($i = 5$); —▲—, $\omega_{1X} = \omega_{3X}$ ($i = 3$); —×—, $\omega_{2X} = \omega_{4X}$ ($i = 3$)].

Table 2), indicating that at low values of applied rate, the natural frequency split is dominated by the split due to the imperfection. At higher applied rates the natural frequency values show a sensibly linear variation with applied rate, similar to that shown in Figure 5. At an applied rate of 10 Hz the split is ∼6·8 Hz. This value is within 1·5% of the split at the same applied rate when the natural frequencies are all initially matched. Therefore, at applied rates that are considerably higher than the initial frequency split, the effects of applied rate dominate the behaviour.

The amplitude ratios for the rotating ring are given by equation (32). It can be seen from Table 9 that at very low input rates ($\Omega_x < 1$ Hz) the amplitude ratios tend to zero or unity: i.e., when there is no input rate the modes involve either in-plane or out-of-plane motion, but not both, as expected. With increasing values of Ω_x the amplitude ratios change and, at higher input rates ($\Omega_x > 10$ Hz) where the input rate dominates the effect of the initial frequency split, they tend towards the values given in Table 2 for the case where there is no difference between the natural frequencies of the in-plane and out-of-plane modes of the non-rotating ring.

TABLE 10

Natural frequencies and amplitude ratios when rate is applied about the in-plane Ox axis when there is a 1 Hz split between the $n = 4$ and $i = 3$ modes of the non-rotating ring

Ω_x (Hz)	$\omega_{1X} = \omega_{3X}$ (Hz)	$\dfrac{\bar{Q}_{I1}}{\bar{Q}_{O1}} = -\dfrac{\bar{Q}_{I2}}{\bar{Q}_{O2}}$	$\omega_{2X} = \omega_{4X}$ (Hz)	$\dfrac{\bar{Q}_{I1}}{\bar{Q}_{O1}} = -\dfrac{\bar{Q}_{I2}}{\bar{Q}_{O2}}$
0	7588·4		7587·4	
1	7588·7	j0·1163 ($\omega_{1X} = \omega_{3X}$)	7587·1	− j0·5545 ($\omega_{2X} = \omega_{4X}$)
5	7590·9	j0·2138 ($\omega_{1X} = \omega_{3X}$)	7585·0	− j0·3015 ($\omega_{2X} = \omega_{4X}$)
10	7593·7	j0·2329 ($\omega_{1X} = \omega_{3X}$)	7582·1	− j0·2767 ($\omega_{2X} = \omega_{4X}$)

Notes: These results apply for the case where $\omega_{I1} = \omega_{I2} = \omega_I$ ($n = 4$) and $\omega_{O1} = \omega_{O2} = \omega_O$ ($i = 3$) and $\omega_O = \omega_I + 1$. Bracketed symbols indicate which solution for the natural frequency is substituted into equation (27). Amplitude ratios are given to four significant figures.

For the case where there is a 1 Hz split between the non-rotating $n = 4$ in-plane frequencies and the $i = 3$ out-of-plane mode frequencies, the natural frequencies and amplitude ratios for the rotating ring are given in Table 10, and the frequency variation is also shown in Figure 7. The pattern of behaviour is the same as that observed for the $n = 4$, $i = 5$ case and, again, at higher input rates, the amplitude ratio values tend to those shown in Table 3.

5. CONCLUSION

The analysis presented in this paper shows that the natural frequencies and mode shapes of a rotating ring structure are affected by components of angular velocity applied about any axis. A vibrating ring structure therefore forms a feasible basis for a rate sensor capable of detecting rate-of-turn applied about three mutually perpendicular axes. This practical application provides the main motivation for the reported work.

Equations of motion are derived for the vibration of a ring which is subjected to angular velocity applied simultaneously about the polar axis and two perpendicular axes in the plane of the ring. Emphasis is placed on the case where the applied rate is much smaller than the flexural natural frequencies of the non-rotating ring. It is shown that angular velocity applied about axes in the plane of the ring couples the in-plane and out-of-plane motion of the ring, and gives rise to complex mode shape vectors. The characteristic equation for the general case is derived and a number of special cases are also considered, for which simple but accurate approximate expressions for the natural frequencies and amplitude ratios are presented.

Due to manufacturing imperfections, there is often a frequency split between the natural frequencies of the non-rotating ring. At applied rates which are of the same order of magnitude as the frequency split, the effects of the initial split are significant. At applied rates which are considerably higher than the initial split, the effects of the frequency split are negligible. The effects of an initial frequency split on the mode shapes are significant for all applied rates.

Numerical examples are presented which quantify the magnitude of the changes in natural frequency and mode shape which result from applied angular velocity.

ACKNOWLEDGMENT

The authors gratefully acknowledge the support for this work provided by BAE SYSTEMS and EPSRC through the Industrial CASE scheme.

REFERENCES

1. I. HOPKIN 1997 *Proceedings of the DGON Symposium on Gyro Technology, Stuttgart*. Performance and design of a silicon micro-machine gyro.
2. L. RISTIC (ed.) 1994 *Sensor Technology and Devices*. London: Artech House.
3. C. H. J. FOX and C. FELL *UK Patent Application GB* 2 335 273 (9/99). A two-axis gyroscope.
4. R. ELEY, C. H. J. FOX and S. MCWILLIAM *Proceedings of I.Mech.E. Part C Journal of Mechanical Engineering Science*, The dynamics of a vibrating-ring multi-axis rate gryoscope. In press.
5. G. F. CARRIER 1945 *Quarterly of Applied Mathematics* **3**, 235–245. On the vibrations of the rotating ring.
6. M. ENDO, K. HATAMUSA, M. SAHATA, O. TANIGUCHI 1984 *Journal of Sound and Vibration* **92**, 261–272. Flexural vibration of a thin rotating ring.
7. W. B. BICKFORD and E. S. REDDY 1985 *Journal of Sound and Vibration* **101**, 13–22. On the in-plane vibration of rotating rings.
8. H. E. WILLIAMS 1987 *Journal of Sound and Vibration* **115**, 65–81. On the in-plane motion of thin, rotating ring segments.
9. R. S. HWANG, C. H. J. FOX and S. MCWILLIAM 1999 *Journal of Sound and Vibration* **220**, 497–516. The in-plane vibration of thin rings with in-plane profile variations, Part I: general background and theoretical formation.
10. C. H. J. FOX, R. S. HWANG and S. MCWILLIAM 1999 *Journal of Sound and Vibration* **220**, 517–539. The in-plane vibration of thin rings with in-plane profile variations, Part II: application to nominally circular rings.
11. R. ELEY, C. H. J. FOX and S. MCWILLIAM 1999 *Journal of Sound and Vibration* Anisotropy effects on the vibration of circular rings made from crystalline silicon, **228**(1), 11–35.
12. C. H. J. FOX 1990 *Journal of Sound and Vibration* **142**, 227–243. A simple theory for the analysis and correction of frequency splitting in slightly imperfect rings.
13. R. D. BLEVINS 1995 *Formulas For Natural Frequencies and Mode Shapes*. New York: Krieger.
14. J. KIRKHOPE 1977 *Journal of Sound and Vibration* **50**, 219–247. In-plane vibrations of thick circular rings.
15. J. KIRKHOPE 1976 *ASCE Journal of the Engineering Mechanics Division*, Vol. 102, 239–247. Out-of-plane vibration of thick circular rings.
16. G. B. WARBURTON 1976 *The Dynamical Behaviour of Structures*. Oxford: Pergamon.

APPENDIX A

The natural frequencies for the non-rotating ring are

$$\omega_{I1}^2 = \frac{K_{I1}(1+\delta k_{I1})}{M_{I1}(1+\delta m_{I1})}, \quad \omega_{I2}^2 = \frac{K_{I2}(1+\delta k_{I1})}{M_{I2}(1+\delta m_{I2})},$$

$$\omega_{O1}^2 = \frac{K_{O1}(1+\delta k_{O1})}{M_{O1}(1+\delta m_{O1})}, \quad \omega_{O2}^2 = \frac{K_{O2}(1+\delta k_{O2})}{M_{O2}(1+\delta m_{O2})},$$

and M_{I1}, etc., and K_{I1}, etc., are the mass and stiffness matrix coefficients from equations (14) and (16) respectively, given as

$$M_I = \rho A a \pi (n^2 + 1), \qquad M_O = \rho A a \pi \left(1 + \frac{J_i^4 \xi^2}{A}\right),$$

$$K_I = \frac{E I_z \pi n^2 (n^2 - 1)^2}{a^3}, \qquad K_O = \frac{i^2 (i^2 - 1)^2 R \pi}{a^3 (1 + i^2 \mu)^2}.$$

G_x, G_y and G_z, are the magnitudes of the coefficients related to Ω_X, Ω_Y and Ω_Z respectively, given as

$$G_X = \rho A a \pi (1 \mp n)_{\substack{n+1=i \\ n-1=i}}, \qquad G_Y = \rho A a \pi (n \mp 1)_{\substack{n+1=i \\ n-1=i}}, \qquad G_Z = 4 n \rho A a \pi.$$

APPENDIX B: NOMENCLATURE

a	ring mean radius (m)
A	cross-sectional area (m^2)
a_l	ring axial length (m)
C_T	torsional coefficient
E	Young's modulus (Pa)
G	shear modulus (Pa)
i	number of out-of-plane nodal diameters
I	second moment of area (m^4)
J	polar second moment of area (m^4)
i, j, k	unit vectors of local co-ordinate system
n	number of in-plane nodal diameters
Q	generalized co-ordinate
$\bar{Q}$	generalized co-ordinate amplitude (m)
r	displacement vector of general point
r_t	radial thickness (m)
T	kinetic energy (J)
U	strain energy (J)
u	out-of-plane displacement (m)
v	in-plane tangential displacement (m)
w	in-plane radial displacement (m)
v_{abs}	absolute velocity of ring element (m/s)
β	angle of misalignment between in-plane and out-of-plane generalized co-ordinates (rad)
μ	stiffness ratio
ϕ	out-of-plane twist of ring section (rad)
θ	angular co-ordinate (rad)
ρ	density (kg/m^3)
ω	natural frequency (Hz)
Ω	applied rate (Hz)

Subscripts

I1	in-plane mode 1
I2	in-plane mode 2
O1	out-of-plane mode 1
O2	out-of-plane mode 2
Ox	axis in the plane of the ring
Oy	axis in the plane of the ring
Oz	axis in the plane normal to the ring
IP	in-plane
OP	out-of-plane